Supporting Information

Lanthanum-induced synergetic carrier doping of heterojunction to achieve high efficiency Kesterite solar cells

Kang Yin [a,c], Licheng Lou [a,c], Jinlin Wang [a,c],Xiao Xu [a,c], Jiazheng Zhou [a,c], Jiangjian Shi [a]*,

Huijue Wu [a], Dongmei Li [a,c,d], Yanhong Luo [a,c,d]*, Qingbo Meng [a,b,c,d]*

[a] *Beijing National Laboratory for Condensed Matter Physics, Institute of Physics, Chinese Academy of Sciences, Beijing 100190, P. R. China*

[b] *Center of Materials Science and Optoelectronics Engineering, University of Chinese Academy of Sciences, Beijing 100049, P. R. China*

[c] *School of Physical Sciences University of Chinese Academy of Sciences, Beijing 100049, P. R. China*

[d] *Songshan Lake Materials Laboratory, Dongguan, Guangdong 523808, P. R. China*

**Corresponding author.*

E-mail: shijj@iphy.ac.cn E-mail: yhluo@iphy.ac.cn E-mail: qbmeng@iphy.ac.cn

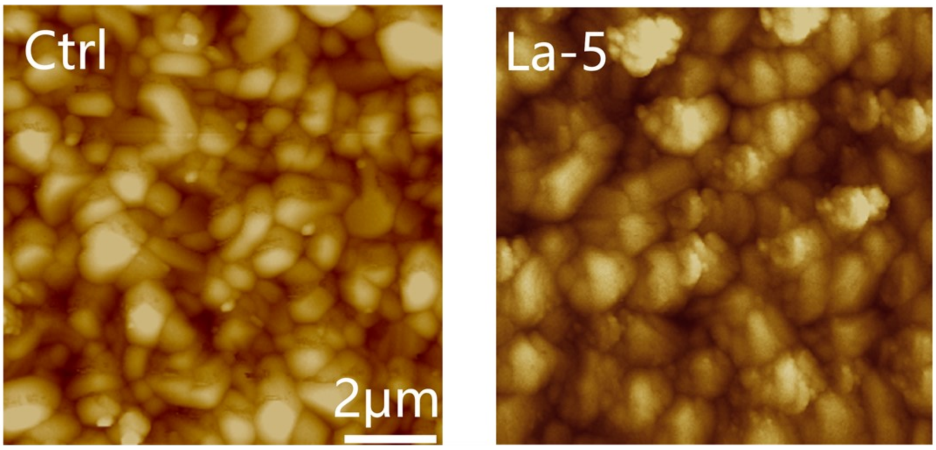

Fig. S1. AFM images of Ctrl and La-5 films.

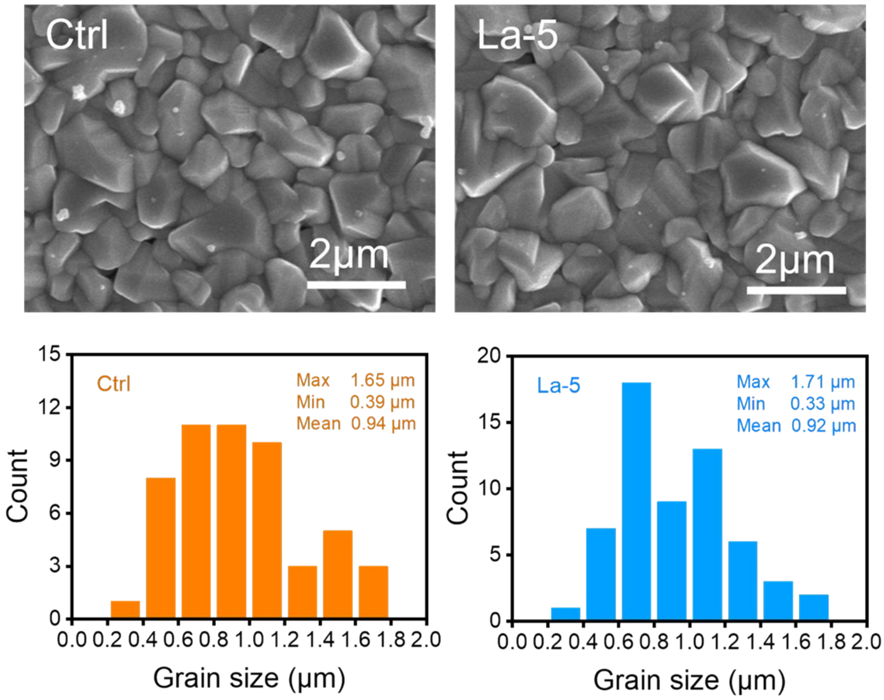

Fig. S2. SEM images of Ctrl and La-5 films and Grain size distribution of those two films. The grain sizes of the Ctrl and La-5 films were mainly 0.6-1.2 microns, and the average sizes were 0.94 and 0.92 microns respectively. This indicates that the grain size does not change significantly after La doping.

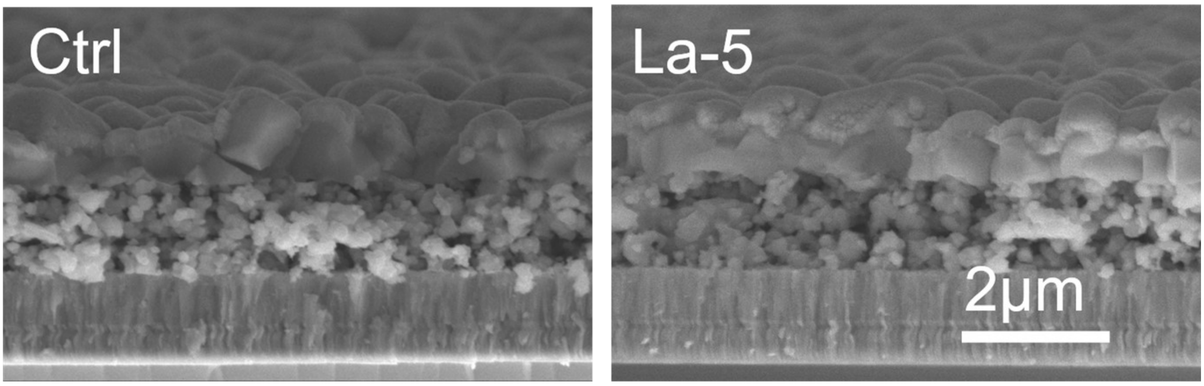

Fig. S3. Cross-sectional-SEM images of Ctrl and La-5 films.

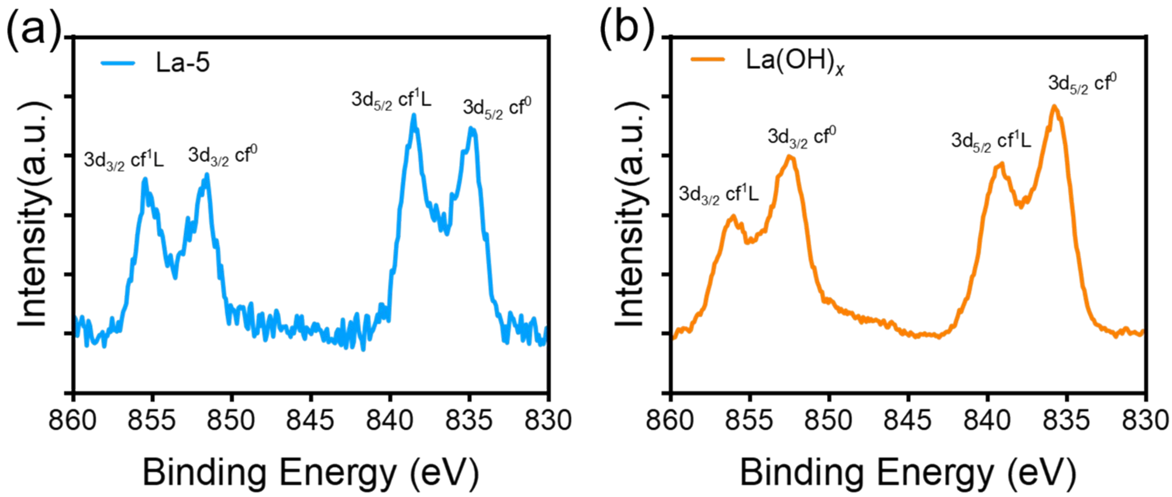

Fig. S4. XPS spectra of La in La-5 film (a) and $La(OH)_3$ powder (b). The peaks at 834 ($3d_{5/2}$ cf^0) and 852 eV ($3d_{3/2}$ cf^0) are attributed to the corresponding two spin−orbits of $3d_{5/2}$ and $3d_{3/2}$, Further, the peaks at 837 ($3d_{5/2}$ cf^1L) and 856 eV ($3d_{3/2}$ cf^1L) can be attributed to the satellite peaks of $3d_{5/2}$ and $3d_{3/2}$ spin−orbits, respectively. According to reported results, for $La(OH)_x$ the ratio of intensity of XPS peaks of La 3d and their satellite peaks f^0/f^1 is greater than 1, but for La_2S_3 the ratio f^0/f^1 is less than 1.[1-4] It could be clearly seen that the f^0/f^1 of La(OH)x is greater than 1 in Fig. S4b. However, for La-5 film, the f^0/f^1 is slightly less than 1. This indicates that part of La possibly diffused from La(OH)x layer to CdS layer and substitute the Cd position in the CdS to form La-S bond.

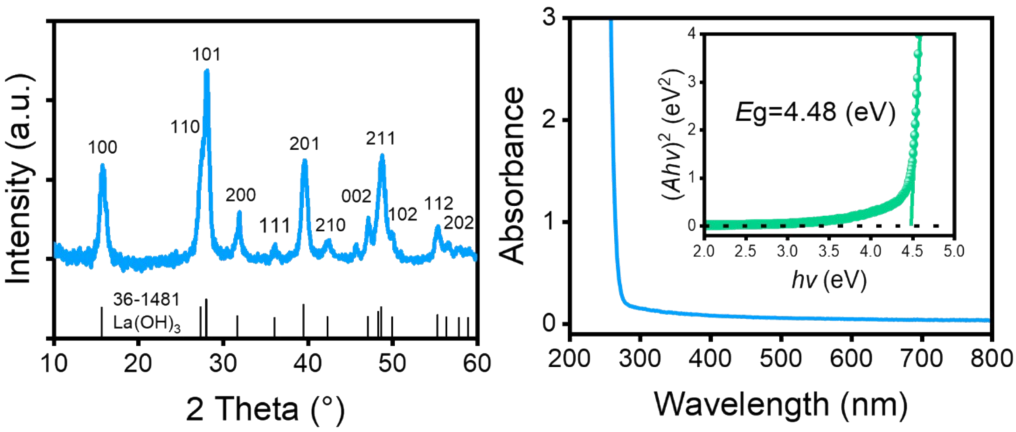

Fig. S5. XRD pattern and UV-Vis absorption spectrum of $La(OH)_3$ powder obtained from mixing $LaCl_3$ and NaOH solutions.

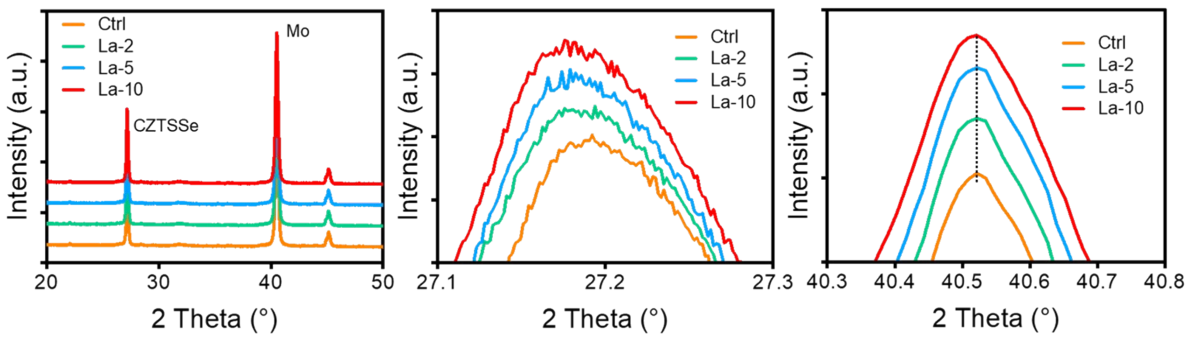

Fig. S6. XRD patterns of control, La-2, La-5 and La-10 films.

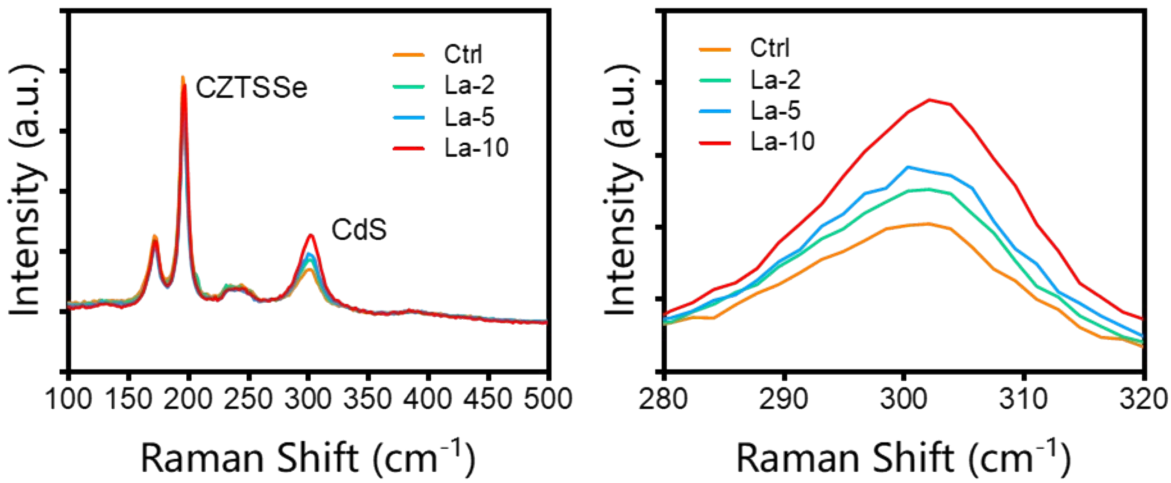

Fig. S7. Raman patterns of control, La-2, La-5 and La-10 films.

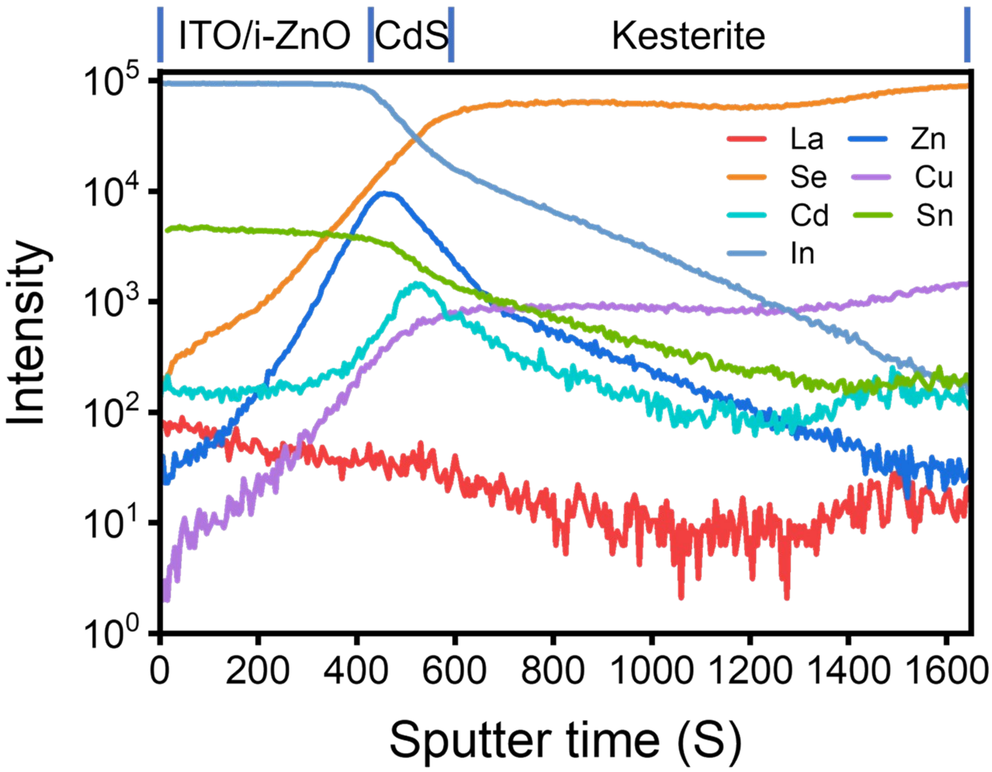

Fig. S8. ToF-SIMS spectra of La-5 devices.

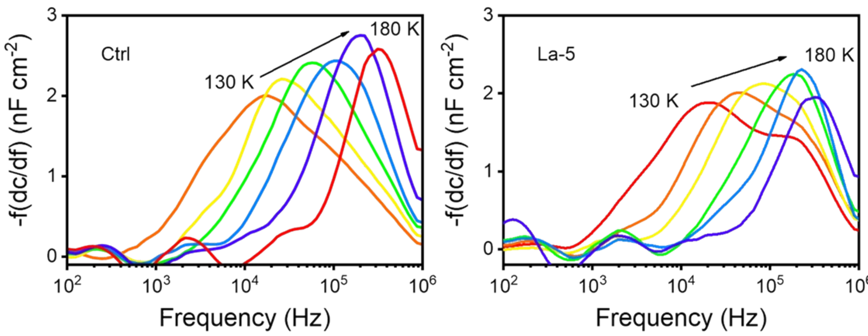

Fig. S9. f vs -f (dC/f) plot from C-f-T spectra of Ctrl and La-5 devices.

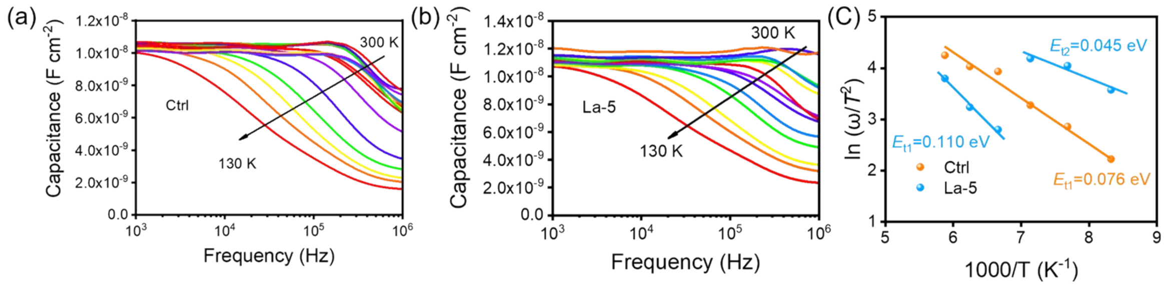

Fig. S10. C-f-T spectra of Ctrl and La-5 device and Arrhenius plots for control and La-5 samples obtained from thermal admittance spectra.

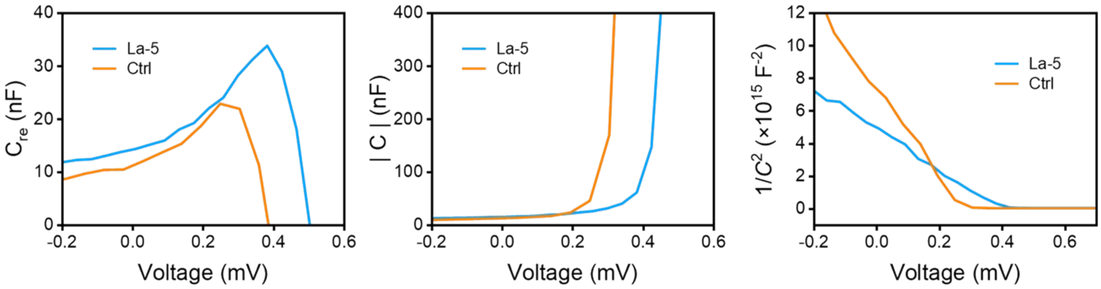

Fig. S11. **C-V curves and Mott-Schottky plot Ctrl and La-5 films.**

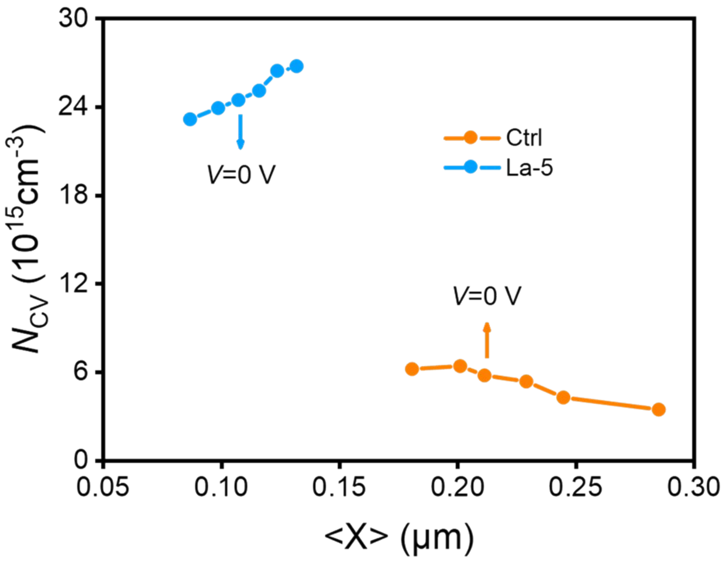

Fig S12. C-V profile of Ctrl and La-5 cells at 100 kHz.

Table S1. Material parameters of different layers for SCAPS-1D simulation.[5-7]

Parameters	ACZTSSe	CdS	CZTSSe/CdS interface	ZnO
Thickness (μm)	1.2	0.05	- -	0.025
Bandgap (eV)	1.1	2.45	- -	3.4
Electron affinity (eV)	4.1	3.7	- -	4.15
Dielectric permittivity (relative)	7	10	- -	10
CB effective DOS (1/cm^3)	2.2*10^{18}	1*10^{19}	- -	1*10^{21}
VB effective DOS (1/cm^3)	1.8*10^{19}	1.5*10^{19}	- -	9*10^{18}
Electron thermal velocity (cm/s)	1*10^7	1*10^7	- -	1*10^7

Hole thermal velocity (cm/s)	$1*10^{7}$	$1*10^{7}$	- -	$1*10^{7}$
Electron mobility (cm^2/Vs)	50	50	- -	$5*10^{-4}$
Holt mobility (cm^2/Vs)	1	20	- -	10
Shallow donor density ND (1/cm^3)	1	$5*10^{17}$ for Ctrl $2*10^{18}$ for La-5	- -	$1*10^{19}$
Shallow acceptor density ND (1/cm^3)	$3*10^{15}$ for Ctrl $1*10^{16}$ for La-5	1	- -	1
Defects	Single acceptor 0.2 eV above E_V $6*10^{15}$ cm^{-2} Single donor 0.3 eV blow E_C $1.5*10^{15}$ cm^{-2}	- -	Single acceptor 0.3 eV above E_V $9*10^{11}$ cm^{-2} for Ctrl $2*0^{11}$ cm^{-2} for La-5	Single donor 0.6 eV above E_V $1*10^{14}$ cm^{-2}

Parameters	MoSe2	Back contact	Front contact	ITO
Thickness (μm)	0.6	- -	- -	0.2
Bandgap (eV)	1.16	- -	- -	3.8
Electron affinity (eV)	4.3	- -	- -	4.6
Dielectric permittivity (relative)	9	- -	- -	10
CB effective DOS (1/cm^3)	$2.2*10^{18}$	- -	- -	$4*10^{18}$
VB effective DOS (1/cm^3)	$1.8*10^{19}$	- -	- -	$9*10^{18}$
Electron thermal velocity (cm/s)	$1*10^{7}$	- -	- -	$1*10^{7}$
Hole thermal velocity (cm/s)	$1*10^{7}$	- -	- -	$1*10^{7}$
Electron mobility (cm^2/Vs)	50	- -	- -	50
Holt mobility (cm^2/Vs)	20	- -	- -	20
Shallow donor density ND (1/cm^3)	1	- -	- -	$1*10^{21}$
Shallow acceptor density ND (1/cm^3)	$3*10^{16}$	- -	- -	1
Thermionic emission / surface recombination velocity (cm/s)		Electrons 10^{5} Holes 10^{7}	Electrons 10^{7} Holes 10^{5}	Single donor 0.6 eV above E_V $1*10^{14}$ cm^{-2}

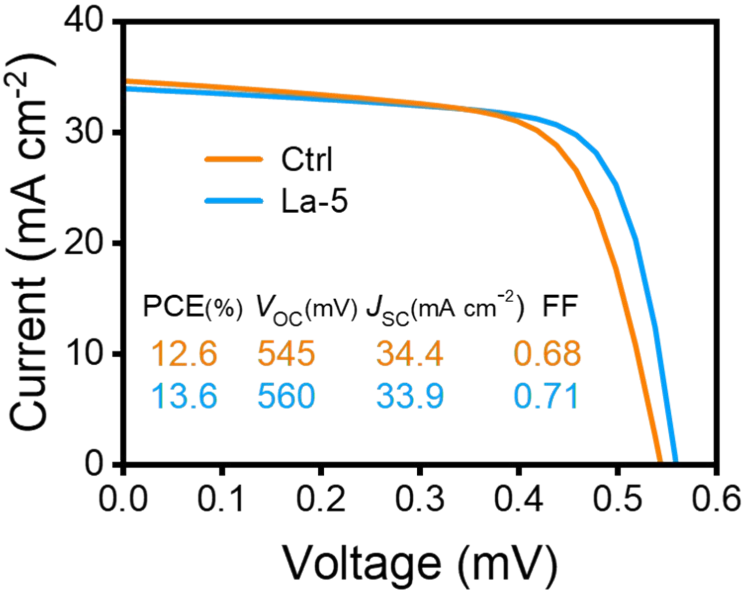

Fig. S13. Simulated *J*-*V* curves by SCPAS with the parameters in table S1.

检测结果/说明：
Results of Test and additional explanation.

1 标准测试条件 STC Standard Test Condition (STC)：

总辐照度 Total Irradiance：1000 W/m^2

被测电池温度 Temperature：25.0 ℃

光谱分布 Spectral Distribution：AM1.5G

2 STC 条件下测量数据

Measurement Data under STC

正扫 Forward Scan

测试次数 Test Times	I_{sc}（mA）	V_{oc}(V)	I_{MPP}(mA)	V_{MPP}(V)	P_{MPP}(mW)	FF(%)	η（%）
1	10.12	0.5494	9.017	0.4281	3.860	69.43	13.63
2	10.11	0.5424	8.974	0.4236	3.801	69.31	13.42
3	10.10	0.5419	8.967	0.4200	3.766	68.81	13.30
平均值 Average Value	10.11	0.5446	8.986	0.4239	3.809	69.18	13.45

反扫 Reverse Scan

测试次数 Test Times	I_{sc}（mA）	V_{oc}(V)	I_{MPP}(mA)	V_{MPP}(V)	P_{MPP}(mW)	FF(%)	η（%）
1	10.12	0.5480	8.900	0.4320	3.845	69.33	13.58
2	10.12	0.5473	8.904	0.4308	3.836	69.26	13.55
3	10.11	0.5471	8.899	0.4280	3.809	68.86	13.45
平均值 Average Value	10.12	0.5475	8.901	0.4303	3.830	69.15	13.53

失配因子 Mismatch factor: 1.010

3 STC 下电流-电压特性曲线和功率-电压特性曲线

I-V & P-V Characteristic Curves under STC

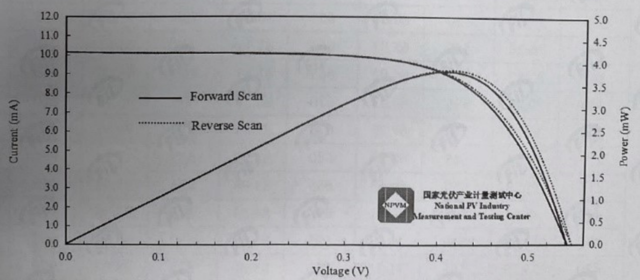

图 1 STC 下电流-电压特性曲线和功率-电压特性曲线
Figure 1. I-V and P-V characteristic curves of the measured sample under STC

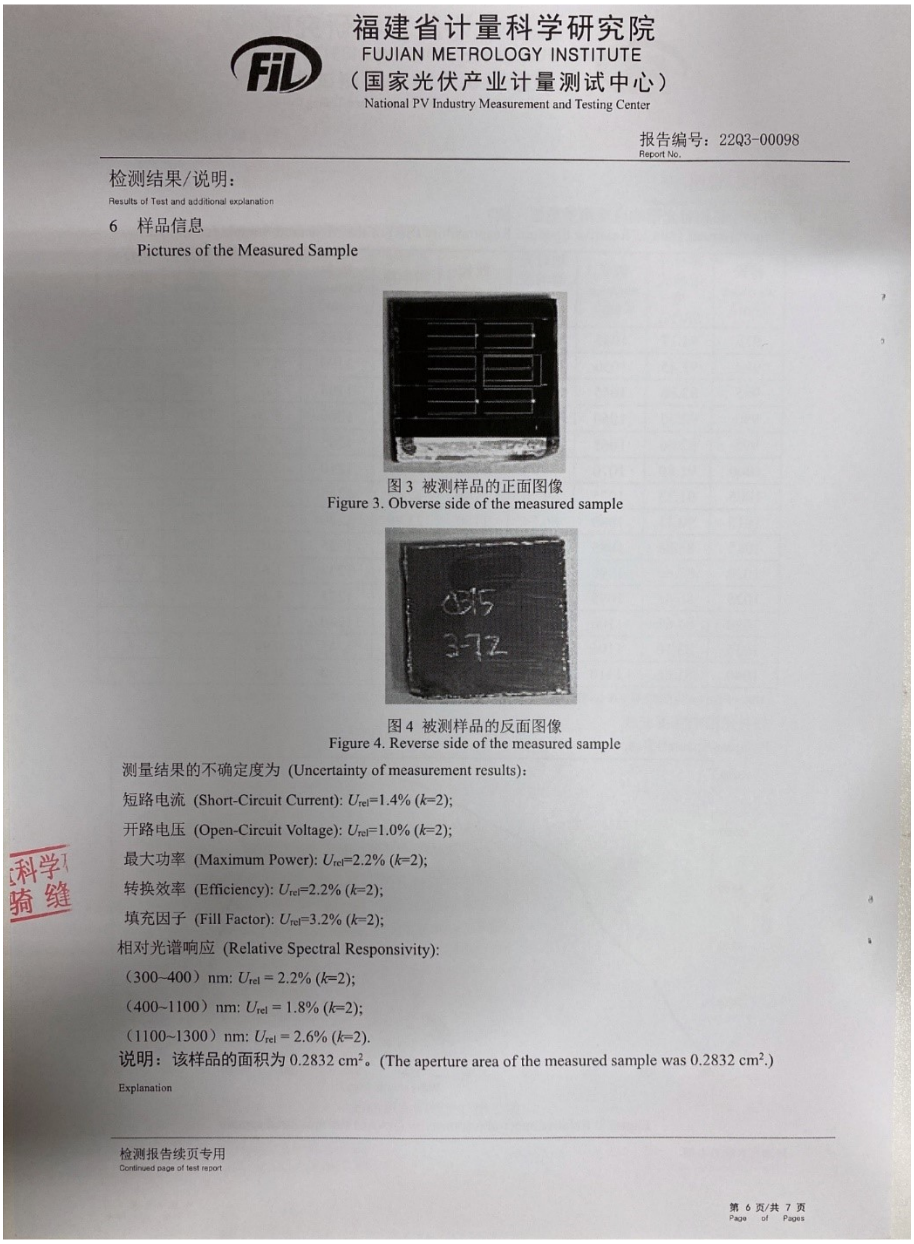

福建省计量科学研究院
FUJIAN METROLOGY INSTITUTE
（国家光伏产业计量测试中心）
National PV Industry Measurement and Testing Center

报告编号：22Q3-00098
Report No.

检测结果/说明：
Results of Test and additional explanation

6 样品信息
Pictures of the Measured Sample

图 3 被测样品的正面图像
Figure 3. Obverse side of the measured sample

图 4 被测样品的反面图像
Figure 4. Reverse side of the measured sample

测量结果的不确定度为 (Uncertainty of measurement results)：

短路电流 (Short-Circuit Current): U_{rel}=1.4% (k=2);

开路电压 (Open-Circuit Voltage): U_{rel}=1.0% (k=2);

最大功率 (Maximum Power): U_{rel}=2.2% (k=2);

转换效率 (Efficiency): U_{rel}=2.2% (k=2);

填充因子 (Fill Factor): U_{rel}=3.2% (k=2);

相对光谱响应 (Relative Spectral Responsivity):

（300~400）nm: U_{rel} = 2.2% (k=2);

（400~1100）nm: U_{rel} = 1.8% (k=2);

（1100~1300）nm: U_{rel} = 2.6% (k=2).

说明：该样品的面积为 0.2832 cm^2。(The aperture area of the measured sample was 0.2832 cm^2.)
Explanation

检测报告续页专用
Continued page of test report

第 6 页/共 7 页
Page of Pages

Fig. S14. Certified test report of the champion CZTSSe solar cell by National PV Industry Measurement and Testing Center (NPVM).

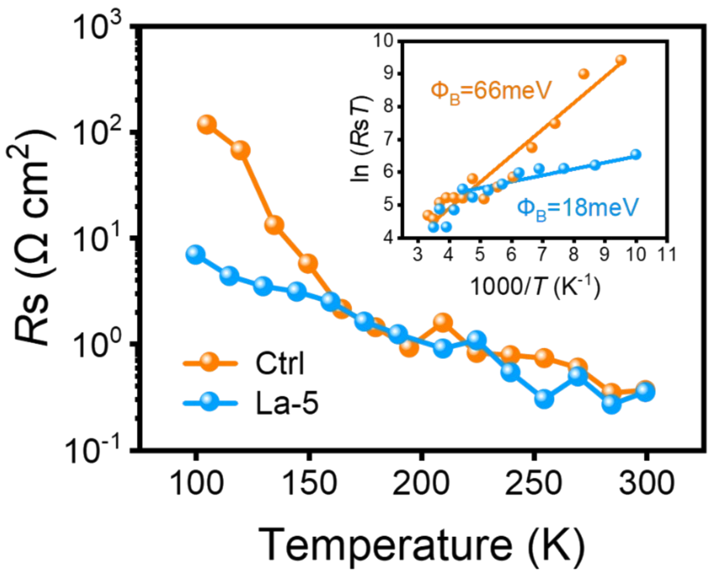

Figure S15. Temperature- dependence Series resistance (Inset: ln(R_ST) vs 1000/T plot) variation of control and La-5 cells. The relative lower carrier barrier potential Φ_B of La-5 cell is consistent of the proper energy band alignment simulated by SCAPS-1D shown in figure 4d.

1. M. F. Sunding, K. Hadidi, S. Diplas, O. M. Løvvik, T. E. Norby and A. E. Gunnæs, *Journal of Electron Spectroscopy and Related Phenomena*, 2011, **184**, 399-409.
2. V. J. Mane, S. B. Kale, S. B. Ubale, V. C. Lokhande, U. M. Patil and C. D. Lokhande, *Journal of Solid State Electrochemistry*, 2021, **25**, 1775-1788.
3. B. Butkus, M. Havel, A. Kostogiannes, A. Howe, M. Kang, R. Gaume, K. A. Richardson and P. Banerjee, *Surface Science Spectra*, 2023, **30**.
4. S. R. Sanivarapu, J. B. Lawrence and G. Sreedhar, *ACS Omega*, 2018, **3**, 6267-6278.
5. J. Li, J. Huang, Y. Huang, H. Tampo, T. Sakurai, C. Chen, K. Sun, C. Yan, X. Cui, Y. Mai and X. Hao, *Solar RRL*, 2021, **5**, 2100418.
6. A. Kumar and A. D. Thakur, *Current Applied Physics*, 2019, **19**, 1111-1119.
7. S. Tripathi, Sadanand, P. Lohia and D. K. Dwivedi, *Sol Energy*, 2020, **204**, 748-760.